Fundamental Interactions of Steels and Nickel-based Alloys with Lead-based Liquid Alloys or Liquid Tin

Carsten Schroer

Abstract The solution of elements from metallic alloys is analysed and compared with observations for steels and nickel-based alloys after exposure to lead-based liquid alloys or liquid tin. Furthermore, the influence of dissolved oxygen and formation of intermetallic compounds are addressed.

Keywords Liquid metal · Corrosion · Solution · Selective leaching · Oxidation · Intermetallic phase

Introduction

Application of lead (Pb)-based liquid alloys or liquid tin (Sn) to thermal energy conversion or storage opens the avenue to compact in design, highly efficient components in the high-temperature section of respective plants, however, at the cost of increased corrosion of metallic materials of construction, namely nickel (Ni)-containing steels or Ni-based alloys. Experimental studies and corresponding theoretical work identify selective leaching of constituent parts, especially Ni, as an intermediate stage of complete dissolution [1], with the near-surface depletion zone originating in the solid alloys being dependent on the alloy composition [2, 3], the liquid metal [3] and temperature [1–3]. If the oxygen content in the liquid allows, formation of solid oxides is likely to interfere with the leaching process or even changes the corrosion mode to oxidation. A similar role intermetallic compound may play.

As to fundamental interactions, the focus is on the transfer to and transport in the liquid metal of dissimilar metals [4]. The dissimilarity primarily refers to the solubility or maximum enrichment the elements may achieve if dissolving from the pure solid, and this solid constitutes the thermodynamically stable solid modification

C. Schroer (✉)
Karlsruhe Institute of Technology (KIT), Institute of Applied Materials—Applied Materials Physics (IAM-AWP), Hermann-von-Helmholtz-Platz 1, 76344 Eggenstein-Leopoldshafen, Germany
e-mail: carsten.schroer@kit.edu

of the element under consideration. However, in the case of metals dissolving from an alloy, concentrations in the liquid metal cannot reach the solubility, except for the element that would remain at the solid/liquid interface after complete leaching of the other elements. Of major alloying elements in steels or Ni-based alloys, the possible enrichment of Ni in liquid metals typically is clearly higher than for iron (Fe) or chromium (Cr), which is illustrated in Fig. 1 for liquid lead–bismuth eutectic (LBE) [5–7].

After analysing the elemental steps that result in the transition of alloying elements to the bulk of the liquid, whilst others stay behind, the theoretical implications are compared to experimental observations. The influence of oxygen dissolved in the liquid metal and the formation of intermetallic compounds are relatively briefly discussed. The observations evaluated with respect to fundamental interactions stem from experiments in Pb-based alloys [1, 3, 8–19] and liquid Sn [20–23] at 400–750 and 500–1000 °C, respectively.

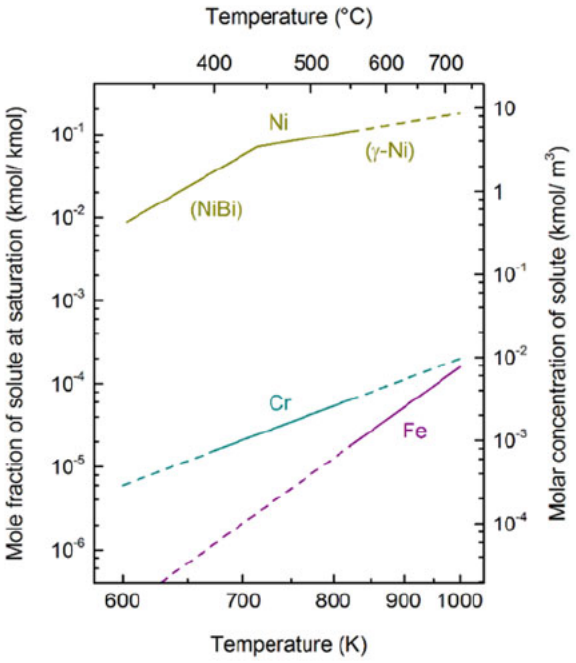

Fig. 1 Solubility of Fe [5], Cr [6] and Ni [6, 7] in LBE as a function of temperature. The solid section of the data plots indicates the temperature range in which experimental data is actually available. It should be noted that at temperature less than about 450 °C, the thermodynamically stable Ni-containing solid is intermetallic NiBi rather than pure nickel [2, 7]. (Color figure online)

Metal Solution and Selective Leaching from Alloys

Analysis of Element Transfer, Transport and Re-Precipitation

The most typical interaction between liquid metals and solid metallic materials certainly is the solution of material elements in the liquid. In the case of alloys, it seems reasonable to assume that the elements initially dissolve in proportion to their concentration in the alloy (general solution of the alloy), so that, after transfer of i mol of alloy to j mol of liquid, the mole fraction x in the liquid is

$$x = \frac{i}{i+j} y + \frac{j}{i+j} x_0 \tag{1}$$

Equation (1) applies to each element with mole fraction y in the solid alloy and initial concentration x_0 in the liquid. A restriction to general solution arises when for one of the alloying elements the thermodynamic activity in the liquid phase approaches that in the solid, or

$$f \times y = \frac{x}{x_s} \tag{2}$$

f is the activity coefficient in the solid corresponding to y, and the inverse of the solubility x_s of the element under consideration replaces the activity coefficient in the ideal diluted liquid solution that is assumed to form. For negligible initial concentrations x_0, inserting Eq. (1) in (2) and rearranging gives

$$i = \frac{f \times x_s}{1 - f \times x_s} j \tag{3}$$

Equation (3) implies $f \times x_s < 1$ ($i, j > 0$), and that the element with smallest $f \times x_s$ (smallest i) first imposes a limit to general solution of the alloy. Especially, in the Cr–Fe–Ni system, activity coefficients in solid alloys seem to be < 5 [2, 24] so that for differences in solubility of more than about half an order of magnitude, it is the alloying element with lowest solubility that is likely to stop general solution. The influence of concentration in the alloy is relatively weak. The criterion for negligible x_0 is

$$\frac{x_0}{f \times y} \ll x_s \tag{4}$$

the violation of which means that the limit to general solution occurs earlier, at smaller i than predicted by Eq. (3). This is again more likely for the element with lowest solubility x_s, and especially if its concentration in the alloy is low.

The process of solution in a certain volume of liquid metal, however, involves not only the transfer across the solid/liquid interface but also diffusion of the transferring elements in the liquid. The analysis so far tacitly assumes that either the liquid volume is small or diffusion fast enough for absorbed elements to disperse uniformly. Any delay in element transport in the liquid leads to accumulation at the solid/liquid interface so that, at this interface, the activity in the liquid approaches the limit earlier. If the diffusion flux into the bulk of the liquid is proportional to the alloy composition just like element transfer in the case of general solution, only the effective volume (j in Eqs. (1) and (4)) becomes smaller, and the equality of activities at the interface is reached earlier. If the diffusion coefficients in the liquid of the transferred elements have similar value, the flux is higher for elements with high concentration in the solid, especially for the parent element of the alloy (generally highest concentration in the liquid at the interface). For the parent element having the lowest solubility in the liquid, this means that another constituent of the solid alloy may equally be responsible for a transition from general to selective solution, possibly the one with the next highest solubility. According to the hydrodynamic approach to diffusion (Stokes–Einstein), the case of similar diffusion coefficients in the liquid is likely to apply to Cr–Fe–Ni alloys, because the atoms have approximately same size. Experimental evidence is available for the diffusion coefficients of Fe and Ni in LBE [25].

At the point of one element prohibiting further solution in proportion to the concentrations in the alloy, something must change. The first and most obvious option is disproportionate, i.e. preferential solution of the other elements that accordingly deplete in the near-surface zone of the solid (depletion zone). At the same time, thermodynamic limits alter with the change in alloy composition, and especially, the element that once has stopped general solution will continue to dissolve as it enriches in the solid at the solid/liquid interface. Furthermore, this element tends to diffuse in the solid towards the bulk of the alloy, whereas the elements that deplete diffuse from the bulk towards the surface. If counterdiffusion is balanced, the surface of the depletion zone recedes rather than porosity develops (Fig. 2a). As diffusion in the solid is likely to be slow in contrast to diffusion in the liquid phase and probably also in comparison with element transfer across the solid/liquid interface. This means, selective solution tends to retard and concentration gradients develop between the bulk of the alloy and the solid/liquid interface. Element transfer across the solid/liquid interface being generally faster than diffusion in the liquid leads to the elements approaching the equality of activity on both sides of the interface one by one. For similar diffusion coefficients in the liquid, the transport away from the interface that is necessary for further solution is relatively fast for elements that are able to enrich in the liquid more than others do, which increases the selectivity of solution for elements with high solubility. The latter naturally applies only if concentrations in the bulk of the liquid are, respectively, low.

Figure 2b extends the view to possible formation of voids in the depletion zone and preferential progress along grain boundaries. Because of crystallographic mismatch between abutting grains and, respectively, stretched or compressed bonds, the atoms at grain boundaries are more likely to transfer to the liquid in contrast to the interior

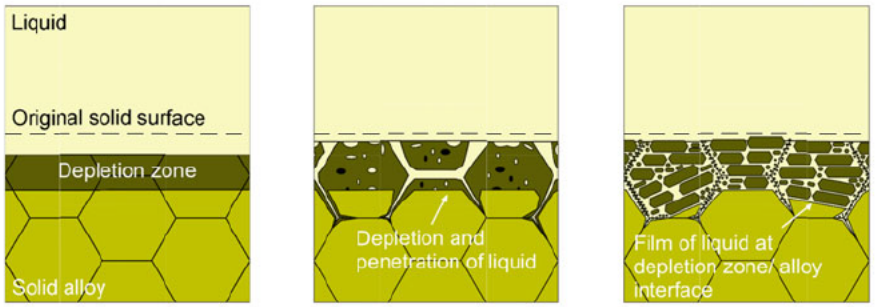

Fig. 2 Schematic illustration of depletion zones as expected to develop in the course of selective leaching for **a** disproportionate element transfer with balanced counterdiffusion in the depletion zone, **b** preferential progress along grain boundaries, and voids forming both at the surface and inside the depletion zone, and **c** re-precipitation of elements of low solubility. (Color figure online)

of the grains. This gives rise to intergranular solution and penetration as especially evident for pure Fe in flowing LBE at 400 [8] and 450 °C [9], but the principle will not change if the material exposed to the liquid is an alloy. In case of disproportionate transfer, the grains deplete in the preferentially transferred elements on both sides of the boundary, and depletion proceeds from this boundary into the adjacent grains. Transport in the finite volume of liquid that penetrates the grain boundary eventually limits further element transfer so that the process of solution retards and the share of intragranular consumption of the alloy gradually increases. However, the notion that solution and especially penetration of the liquid have begun at grain boundaries may persist. Relatively slow diffusion of the elements of low solubility towards the unaffected alloy, i.e. fast diffusion of highly soluble elements in the opposite direction, is likely to maintain voids in the surface as well as create porosity inside the depletion zone. The higher the porosity inside the depletion zone, the smaller the (average) surface recession, which equally applies to concentration in the solid of elements of high solubility being high or low. Pores may allow the liquid to penetrate the depletion zone in addition to the grain boundaries. But the necessary prerequisite for the liquid reaching the alloy in original composition by this means is a continuous network of pores crossing the depletion zone.

The alternative to dispersion in the bulk of the liquid is re-precipitation, possibly after some short-range diffusion [1]. Re-precipitation of elements nearby the site of solution necessitates that, through solution from the alloy, these elements achieve a concentration or activity in the liquid that is higher than in a solid phase that may newly form. For precipitation of a pure solid element, this means enrichment to above solubility or activity >1, whereas the required element activity is lower if an alloy precipitates. Activity >1 in the liquid implies activity >1 also in the original solid alloy that, for the primarily settled element, then is a metastable modification such as austenite for Fe at temperature less than about 900 °C. Thermochemical data suggests a value of 1.2 for Fe activity in hypothetic pure γ–Fe (austenite) at

800 K (527 °C) [26], a temperature at which α–Fe (ferrite) clearly is the stable modification. If re-precipitation at a minimum of diffusion is an option especially for elements that have only low solubility in the liquid, they are less likely to restrain proportional transfer across the solid/liquid interface. In this case, the depletion zone does not originate from disproportionate solution as such but through precipitation along with dispersion in the liquid of those elements that enter the newly formed solid in only minor amounts. This solid being interspersed with the liquid is inherent to the formation mechanism, and a thin layer of liquid separating it from the original alloy is probably characteristic [1]. Allotropic transformation, however, is not an exclusive feature of re-precipitation, but possible also if the elements stabilising a metastable original alloy preferentially transfer to the liquid.

Figure 2c illustrates the re-precipitation of elements of low solubility after element transfer to the liquid in proportion to the alloy composition. The grain boundaries are again the sites where the processes most likely start. Necessary element transport, especially of the highly soluble alloying elements, in the liquid volume that penetrates the grain boundaries is hampered by the first precipitates of the newly formed phase. Consequently, the solution and subsequent precipitation on the grain face gain in importance. The precipitates above the interior of the grains are likely to be large in comparison with particles forming at and especially inside the limited space along grain boundaries, so that the original alloy microstructure is traced through small between large precipitates. Growth of large at the cost of small particles (Ostwald ripening) may clear the former grain boundaries from precipitates, by which the original alloy structure becomes even more apparent in the depletion zone. In contrast to depletion by disproportionate transfer to the liquid, there is no diffusion towards the alloy of the elements remaining in the depletion zone, because their activity in the precipitating solid is at most equal if not less than in the alloy. Accordingly, for the surface of the depletion zone to recede, repeated transfer to and dispersion in the liquid are required [1]. As mentioned above, the presence of a newly formed phase is not distinctive for the re-precipitation mechanism. It rather is the missing depletion below the deepest penetration of the liquid that excludes disproportionate element transfer to the liquid. A film of liquid separating precipitated particles from the alloy is a necessary indication for short-range diffusion in the liquid before precipitation, but also establishes if nucleation occurs immediately on the alloy surface and further solution proceeds around the formed particle. The latter is an option especially in the initial stage, whereas, in the long run, the growth of the existing particles is likely to be more favourable.

Observations from Experiments

A large part of experimental investigations in which material solution in liquid metal is evident has been performed on steels. Significantly different solubility of the major alloying elements, as illustrated in Fig. 1 for LBE, especially occurs in the case of austenitic grades. At moderately high temperature, namely <900 °C, ferrite is the

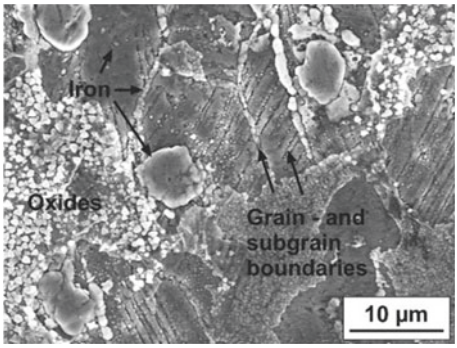

Fig. 3 Surface of 15–15 Ti steel 1.4970 (40% cold work, flat surface, polished) after exposure for about 5000 h to flowing LBE at 400 °C and 10^{-7}% dissolved oxygen [10]

generally more stable modification of the parent element of the alloy, so that, from the purely thermodynamic point of view, selective element transfer or the precipitation primarily of Fe is equally likely to occur. An indication of the latter (Fig. 3) has been found in 15–15 Ti steel 1.4970 after exposure to flowing LBE at 400 °C, on the flat, polished surface of the material both in the solution annealed and cold-worked (40%) state [10]. In the particular experiment, the LBE contained 10^{-7}% (by mass) oxygen so that the solution typical for the interaction with liquid metal competes with surface oxidation. Figure 3 constitutes an early stage of solution that has started after a period dominated by the formation of surface oxides. As other materials, especially technically pure Fe [8], have been tested in the same experimental run, it may not be excluded that the accumulated Fe has partially deposited from the flowing liquid metal, the temperature of which may (slightly) decrease as it passes the exposed samples one after another. However, the interaction of the austenitic steel and the liquid metal is obvious from cross-sectional analyses, especially for grain and subgrain boundaries [10], and re-precipitation of Fe seems all the more required for maintaining proportional element transfer from the steel if the Fe concentration in the liquid is already high.

Figure 3 also exhibits indications of preferential attack along grain and subgrain boundaries. Accelerated element transfer and liquid–metal penetration facilitated by high local defect density in the solid are generally more likely to occur at high-angle grain boundaries, for which the crystallographic mismatch of the neighbouring grains certainly is largest. However, solution and penetration may be clearly more apparent along subgrain boundaries, most notably the deformation twins in cold-worked austenitic steels that have been exposed to LBE at 450 [11] or 500 °C [12]. While highest potential energy or highest mobility of atoms cannot immediately explain this striking observation, the formation of low-energy liquid/solid interfaces possibly favours the penetration of liquid into a subgrain boundary if this boundary divides the grain parallel to crystallographic planes with special affinity to the liquid. Along former twin boundaries and where the latter would intersect each other, electron microscopy [11] reveals ferrite with reduced Ni and Cr content in comparison with the original steel, always enclosed by solidified LBE. Transport of Ni and Cr in the penetrated liquid is evident, whereas element depletion on the side remote

from the ferrite is not apparent from the presented elemental maps and other micro-analyses, and not particularly addressed in the evaluations. A mechanism has been proposed for depletion and transformation into ferrite of narrow twins of submicron thickness, starting with penetration of the liquid metal along two almost adjacent twin boundaries [11]. The idea that a narrow austenite twin widens through selective leaching of elements, which opens the space for further ingress of liquid metal [11], may apply analogously for a single twin boundary, considering the loss of material in connection with the removal of atoms via the penetrating liquid. An advanced state of selective leaching in austenitic steel is exemplified in Fig. 4 that stems from experiments in oxygen-containing flowing LBE at 550 °C [13]. Liquid metal that has penetrated the depletion zone seems to trace at least a part of the grain boundaries in

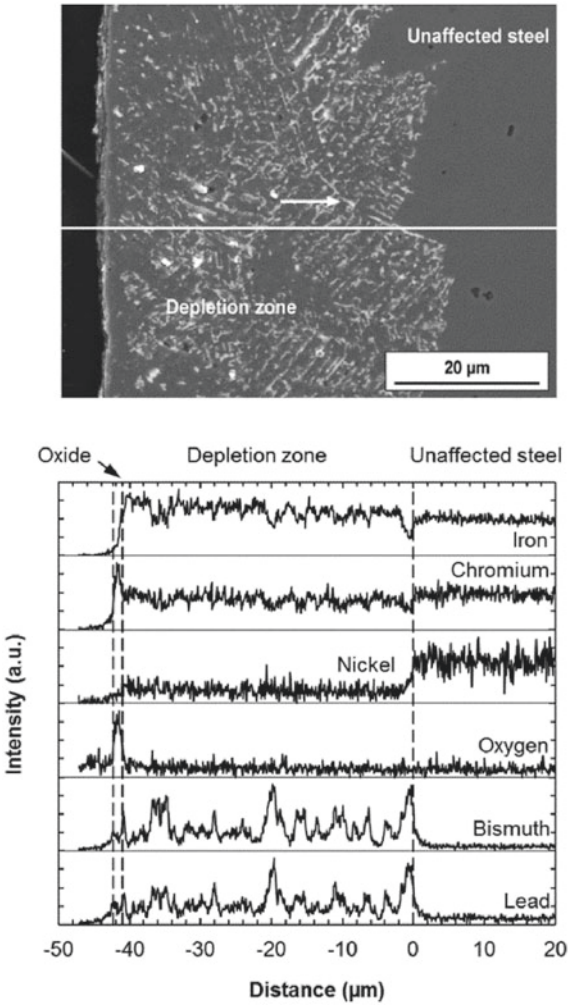

Fig. 4 Cross section of a depletion zone that has formed in austenitic steel 1.4571 during exposure for 5012 h to oxygen-containing flowing LBE at 550 °C [13]

the original microstructure of the steel, but progress at the depletion zone/steel interface is largely transgranular. The results from energy-dispersive *X*-ray spectroscopy (EDS) performed across the near-surface portion of the steel imply that depletion is confined by the deepest penetration of the liquid metal. The particular shape of the depletion zone/steel interface depends on temperature [1], the concentration and orientation of deformation twins in the material [12] or other special features of the microstructure of the steel [14]. The formed surface oxide (Fig. 4) may have retarded [1] but could obviously not suppress selective leaching.

Most notably if the oxygen concentration (activity) in the liquid metal suffices to stabilise oxides of the material elements, solution needs an incubation period during which surface oxides are destroyed. For austenitic steel exposed to static LBE at 500 °C [3] or flowing LBE at 400–550 °C [15], the kinetics of the processes that then take place may initially be described by a linear rate law. In the long run, however, the instantaneous velocity with which selective leaching consumes the steel decreases with time [1, 14]. The duration of apparently linear degradation depends on temperature and the specific austenitic material under consideration [15]. Albeit different in the quantitative outcome, weight change as a function of time determined at 700 °C in flowing sodium (Na) corroborates that, on average, the rate of selective leaching decreases with time for various austenitic steels [27–29]. The identification of the rate determining elemental step in the overall process naturally depends on the mechanism that is presumed being active, but, as a basic principle, it must be the slowest of the subprocesses that are necessary to maintain element transfer from the solid to the liquid phase. For selective element transfer, this would be either diffusion in the gradually depleting steel towards or transport of the preferentially dissolving elements in the liquid. A network of former grain boundaries and, possibly, pores that are penetrated by the liquid (Fig. 2b) reduces the distance to cover by means of diffusion in the solid state. In the case of the re-precipitation mechanism (Fig. 2c), again the transport in the liquid phase imposes a limit on continuing (non-selective) element transfer, but, in the effect of removing dissolved elements from the liquid at the site of dissolution, is supported by the precipitation of the elements of low solubility [1]. Finally, it cannot be excluded that depending on local pre-requisites for dispersion via the liquid (thickness of liquid films), resupply through diffusion in the depleting solid (microstructure, element concentration) or re-precipitation (available space) temporarily take turns, which seems all the more likely if selective leaching preferentially proceeds along grain boundaries or narrow subgrains. In general, however, non-selective element transfer along with re-precipitation should enable faster progress, because it works without solid-state diffusion [1]. Austenitic steels are predestined to gradually dissolve according to this mechanism especially at temperature at which austenite is the metastable solid modification of Fe.

Austenitic steel exposed to liquid Sn [20] shows ferrite formation only at >650 °C and most notably at >840 °C. Both Cr in the steel and Sn stabilise the ferritc phase that is still observed at >1050 °C. At >1050 °C, not only the surface recession of the depletion zone becomes prominent but also the formed ferrite tends to recrystallise into a continuous layer. Additionally, a preference for Ni removal and phase transformation near twins in the austenitic structure is found. The habitus of ferrite

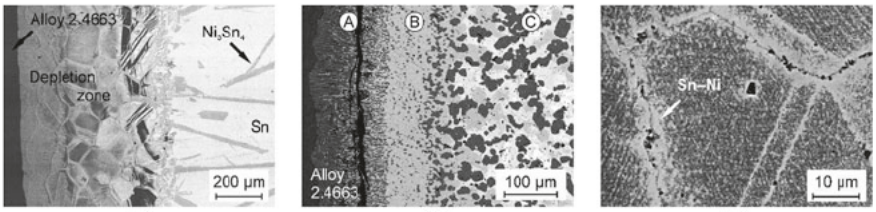

Fig. 5 Selective leaching in Ni-based alloy 2.4663 (Ni–22Cr–12Co–9Mo) after contact with static liquid Sn **a** for 25 h at 700 °C and **b** for 50 h at 1000 °C. **c** Detail of the innermost part of the depletion zone in Fig. 5a [21]

changes from globular to columnar if conditions are adverse to the removal of Ni, i.e. after pre-saturation of the liquid with Ni, for comparatively small volume of liquid or decreasing temperature. Ferrite interspersed with liquid is most obvious in the temperature range from 950 to 1050 °C and occurs for both shapes of ferrite grains. Especially at <950 °C, the austenite at the interface with columnar ferrite does not show Ni depletion [20], which complies with slow Ni transport in the austenite in contrast to diffusion across the ferritic zone even in the absence of penetrated liquid. Besides the presence of intermetallic compounds, e.g. Ni_3Sn_2 that seems to have formed at up to 1050 °C [20], Sn entering and stabilizing the ferritic phase is likely to influence the detailed mechanism of ferrite formation. At >900 °C, solid-state diffusion becomes increasingly faster, whereas the precipitation of Fe-rich ferrite from the liquid is rather improbable.

Figure 5 presents examples of selective leaching in Ni-based alloy as observed after exposure to static liquid Sn at 700 and 1000 °C, respectively [21]. At 700 °C (Fig. 5a), the body of the depletion zone mainly consists of a conglomerate of Sn–Ni and Cr–molybdenum (Mo) phases. The Sn–Ni part is likely to be at least partially liquid at 700 °C, whereas Cr and Mo are major alloying elements of low solubility in the particular Ni-based material. The microstructure of the original alloy is largely conserved. In the outer portion, Cr–Mo has more clearly separated from Sn–Ni and accumulated in the domains that appear dark in the backscatter electron (BSE) micrograph depicted in Fig. 5a. The latter certainly results from ageing of the depletion zone. At 1000 °C (Fig. 5b), three subzones can be distinguished: (A) the innermost part, showing columnar Cr–Mo interspersed with Sn–Ni; (B) a transition zone characterised by high percentage of Sn–Ni and small particles that seem to have originated from disintegration of the columnar Cr–Mo in subzone A; and (C) comparatively large particles enclosed by Sn–Ni. The large particles have gained in size partly through absorption of Fe from the liquid Sn [21]. The most obvious difference between the two scales is the percentage of Sn–Ni via which Ni and other alloying elements of rather high solubility in Sn, such as cobalt (Co), defect from the original alloy. Columnar Cr–Mo formed at 1000 °C is reminiscent of the ferrite structure attributed to relatively low velocity of Ni transfer to the bulk of the liquid metal [20]. At 300 °C lower temperature, at which the original microstructure of

the alloy is conserved, not only the rate of element removal is significantly reduced but also the capacity of the liquid Sn for dissolving Ni as well as other alloying elements is clearly lower. Both favour elements of low solubility staying behind in the depletion zone. The re-precipitation mechanism could explain the generally fine dispersion but accumulation of Sn along the grain boundaries of the original alloy (Fig. 5c), and precipitation of Cr–Mo after transport only over a short distance would comply with reproduction of the original microstructure.

Influence of Dissolved Oxygen

At the time of the first exposure to the liquid metal, the surface of solid metallic materials is rarely clean in the sense that there is no adsorption layer or precursor of a surface scale formed during storage and handling. Surface oxides are of particular importance in this respect. Depending on the oxygen concentration, or more precisely, oxygen activity in the liquid metal, they tend to degrade, grow or transform. Surface oxide that is stable under the prevailing conditions may effectively suppress the interaction with the liquid metal [16]. However, along with growth of an oxide film, defects accumulate which renders the oxide prone to local failure [30, 31], i.e. the interaction with the liquid metal is only delayed [17] rather than completely avoided.

The influence of oxygen that is dissolved in the liquid metal is not confined to the formation of surface oxides. Where such an oxide scale remains discontinuous or locally loses its protective properties, solid oxides may also form after transfer of the respective material element to and transport in the liquid metal. This gives rise to the precipitation of oxide in some distance from the site of element solution as, e.g., observed for austenitic steel at 450 °C in the presence of static LBE containing 10^{-7}% oxygen [17]. The formation of solid oxide is an alternative way of a dissolved element leaving the solution, and the concentration of this element in the liquid is rather low at the site where the precipitation occurs. Accordingly, concentration gradients become steeper which supports element transport and, therefore, further solution from the solid alloy. For selective leaching this means, oxidation improves the conditions for transport in the liquid specifically for oxide-forming elements, which suggests oxidation of Fe and Cr as an explanation for different ferrite contents in depletion zones formed in austenitic steel at 450 and 550 °C, in flowing LBE with 10^{-6}% dissolved oxygen in both cases [1]. Likewise, lower Cr content in the depletion zone and overall higher material loss have been attributed to higher oxygen activity in Pb–lithium (Li) alloys with different Li concentrations [18]. Oxide formation may even reverse the situation as to selective leaching in the sense that elements with generally high solubility stay in the alloy, whilst elements of low solubility preferentially transfer to the liquid and subsequently precipitate. An example is the performance of binary Ni–Cr alloys, especially Ni with 35% Cr in static liquid Pb at 750 °C and 10^{-6}% dissolved oxygen [19]. The EDS linescan presented in Fig. 6 indicates near-surface enrichment of Ni, and Cr depletion in the alloy, although Ni

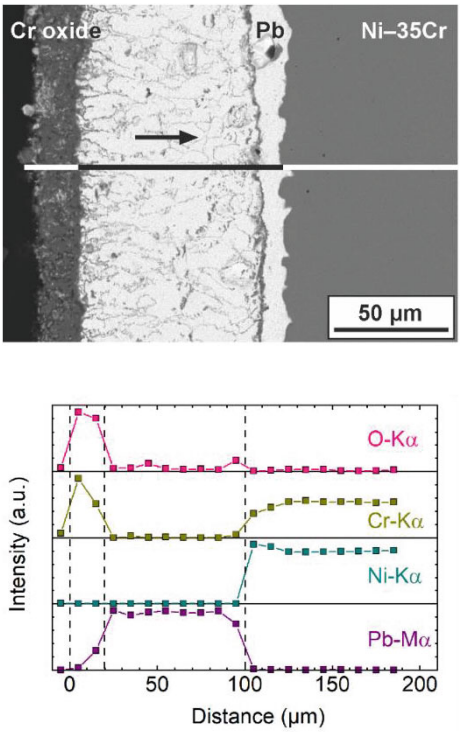

Fig. 6 Ni–35Cr model alloy after exposure for 120 h to oxygen-containing static Pb at 750 °C: BSE micrograph and results of qualitative EDS analyses performed along the indicated line [19]. (Color figure online)

solubility in Pb is clearly higher than the solubility of Cr [32]. Cr has re-precipitated to form an oxide layer that finally encloses the liquid metal.

Oxygen enrichment above the threshold for the formation of oxides of the alloying elements in steels and Ni-based alloys is also possible for liquid Sn, giving rise to suppression of element solution as well as only local occurrence of solution [22].

Formation of Intermetallics

The formation of intermetallic compounds is particularly important in the Fe–Sn [33] and Ni–Sn systems [34]. At temperature in the range of 500 °C, Ni in austenitic steel primarily transfers to the liquid metal, but a significant share of Fe is retained as $FeSn_2$, and FeSn to lesser extent, in a solid surface scale on the steel [21–23]. Consumption of the steel is non-selective, which changes, if temperature increases to around 700 °C. Furthermore, austenitic steels now develop the depletion zone at the instantaneous surface that is typical for selective leaching especially of Ni. The removal of Ni is likely to still occur through a solid intermetallic layer that, in this temperature range, predominantly consists of FeSn [21–23]. This layer is interspersed with particles that are rich in Cr and Mo. Their Fe content and size decrease with

increasing distance from the alloy [21]. Ferrite that has formed in the depletion zone is columnar, similar to Fig. 5b, and the notion that the particles enclosed by FeSn have separated from the columnar ferrite equally arises. The removal of Ni through the intermetallic layer requires an adequate solubility in $FeSn_2$ or FeSn and is driven by the high solubility of Ni in liquid Sn. Ni–Sn intermetallics alternatively form if the bulk of the liquid is Ni-saturated. In pits originating from local initiation of the interaction with liquid Sn, Cr–Mo forms a network, as the ratio of Sn available inside the pit and active alloy surface area is rather small [22].

Also in the case of Ni-based alloys, the stability of intermetallic compounds with Sn changes the initially liquid Sn/solid alloy interaction into a solid/solid interaction with Ni_3Sn_4 being the dominant intermetallic at 700 °C [21, 22]. As the growth of Ni_3Sn_4 primarily consumes Ni, the qualitative outcome, i.e. formation of a conglomerate of Sn–Ni and Cr–Mo similar to Fig. 5c, does not significantly change in comparison with selective leaching caused by liquid Sn, but the consumption of material is clearly lower if there is a Ni_3Sn_4 layer on the surface, as experiments with Ni-saturated Sn show [22]. The solubility of Cr and Mo in the intermetallic may be equally low or even lower than in liquid Sn, and diffusion of these elements is slower. At high concentration of Fe in the alloy and temperature at which Fe–Sn intermetallics are stable, the formation of the latter competes with the development of ferrite that, for austenitic steel, completely vanishes at 500 [21, 22] or the amount of which is reduced at 700 °C [21, 22].

In contrast to liquid Sn, the formation of intermetallic phases plays a negligible role in the performance of steels or Ni-based alloys in the presence of liquid Pb or LBE. This especially applies to the typical temperatures of interest. However, precipitation of the bismuth (Bi)–Ni intermetallics NiBi or $NiBi_3$ is to be taken into account if LBE absorbs Ni from materials in a non-isothermal system.

Conclusions

The analysis of dissimilar metal transfer from a solid alloy to the bulk volume of a liquid shows that the process becoming selective for certain alloying elements depends on the solubility of the metals under consideration, but only weakly on their concentration in the alloy. The re-precipitation of elements of low solubility is generally favoured over disproportionate transfer to the liquid if, for the re-precipitating elements, the alloy is not the thermodynamically most stable modification under the prevailing conditions such as austenite in the case of Fe at <900 °C. This especially applies to temperature too low for significant diffusion in solids. Re-precipitation is indicated by a film of liquid separating a zone depleted in the elements of high solubility from the alloy in its original composition.

Experimental observations as to selective leaching are more numerous for austenitic steel and Pb-based alloys, most notably LBE, if compared with Ni-based alloys or liquid Sn. The results from high-resolution microscopy available for narrow twins [11] show the characteristics of re-precipitation most clearly, for austenitic steel

after exposure to LBE at 450 °C. Selective leaching caused by Sn without influence of the formation of intermetallic phases is to be expected at temperatures high enough for remarkable solid state diffusion, so that one of the main arguments against disproportionate solution loses validity. Furthermore and unlike Pb or Bi, Sn contributes to the ferritic phase that is the product of the decomposition of austenitic steels [20], so that same mechanism of selective leaching as in LBE at moderately high temperature is not a matter of course. The identification of re-precipitation as the prevailing mechanism for Ni-based alloy and Sn at 700 °C has, at this stage, preliminary character and partly bases on the contrast to observations at 1000 °C.

Dissolved oxygen supports leaching of elements that form solid oxides. The formation of intermetallic compounds of alloying elements that exhibit high solubility in the liquid metal reduces the rate of selective leaching, but apparently has weak influence on the structure of the depletion zone that develops. The latter is in contrast to elements of low solubility forming intermetallics with the constituent parts of the liquid metal.

References

1. Schroer C, Wedemeyer O, Novotny J et al (2014) Selective leaching of nickel and chromium from Type 316 austenitic steel in oxygen-containing lead–bismuth eutectic (LBE). Corros Sci 84:113–124
2. Gossé S (2014) Thermodynamic assessment of solubility and activity of iron, chromium, and nickel in lead bismuth eutectic. J Nucl Mater 449(1–3):122–131
3. Yamaki E, Ginestar K, Martinelli L (2011) Dissolution mechanism of 316L in lead–bismuth eutectic at 500°C. Corros Sci 53(10):3075–3085
4. Manly WD (1956) Fundamentals of liquid metal corrosion. Corrosion 12(7):336t–342t
5. Weeks JR, Romano AJ (1969) Liquidus curves and corrosion of Fe, Ti, Zr and Cu in liquid Bi–Pb alloys. Corrosion 25(3):131–136
6. Rosenblatt G, Wilson JR (1970) The solubilities of several transition metals in liquid lead–bismuth eutectic. In: Draley JE, Weeks JR (eds) Corrosion by liquid metals: proceedings of the sessions on corrosion by liquid metals of the 1969 Fall meeting of the Metallurgical Society of AIME, October 13–16, 1969, Philadelphia, Pennsylvania. Plenum Press, New York, London, pp 469–477
7. Martinelli L, Vanneroy F, Diaz Rosado JC et al (2010) Nickel solubility limit in liquid lead–bismuth eutectic. J Nucl Mater 400(3):232–239
8. Schroer C, Tsisar V, Durand A et al (2019) Corrosion in iron and Steel T91 caused by flowing lead–bismuth eutectic at 400 °C and 10^{-7} mass% dissolved oxygen. J Nucl Eng Radiat Sci 5(1)
9. Schroer C, Skrypnik A, Wedemeyer O et al (2012) Oxidation and dissolution of iron in flowing lead–bismuth eutectic at 450 °C. Corros Sci 61:63–71
10. Tsisar V, Schroer C, Wedemeyer O et al (2018) Effect of structural state and surface finishing on corrosion behavior of 1.4970 austenitic steel at 400 and 500 °C in flowing Pb–Bi eutectic with dissolved oxygen. J Nucl Eng Radiat Sci 4(4)
11. Hosemann P, Frazer D, Stergar E et al (2016) Twin boundary-accelerated ferritization of austenitic stainless steels in liquid lead–bismuth eutectic. Scripta Mater 118:37–40
12. Klok O, Lambrinou K, Gavrilov S et al (2018) Effect of deformation twinning on dissolution corrosion of 316L stainless steels in contact with static liquid lead–bismuth eutectic (LBE) at 500 °C. J Nucl Mater 510:556–567

13. Schroer C, Wedemeyer O, Novotny J et al (2011) Long-term service of austenitic steel 1.4571 as a container material for flowing lead–bismuth eutectic. J Nucl Mater 418(1–3):8–15
14. Lambrinou K, Charalampopoulou E, van der Donck T et al (2017) Dissolution corrosion of 316L austenitic stainless steels in contact with static liquid lead–bismuth eutectic (LBE) at 500 °C. J Nucl Mater 490:9–27
15. Tsisar V, Schroer C, Wedemeyer O et al (2016) Long-term corrosion of austenitic steels in flowing LBE at 400 °C and 10^{-7} mass% dissolved oxygen in comparison with 450 and 550 °C. J Nucl Mater 468:305–312
16. Asher RC, Davies D, Beetham SA (1977) Some observations on the compatibility of structural materials with molten lead. Corros Sci 17(7):545–557
17. Klok O, Lambrinou K, Gavrilov S et al (2018) Effect of lead-bismuth eutectic oxygen concentration on the onset of dissolution corrosion in 316 L austenitic stainless steel at 450 °C. J Nucl Eng Radiat Sci 4(3):31019
18. Barker MG, Coen V, Kolbe H et al (1988) The effect of oxygen impurities on the behaviour of type 316 stainless steel in Pb–17Li. J Nucl Mater 155–157:732–735
19. Picho O (2014) Beständigkeit von Nickel-Chrom-Legierung und Eisenaluminidschichten in sauerstoffhaltigen flüssigen Bleilegierungen. Karlsruhe. https://doi.org/10.5445/IR/1000043553
20. Duc D, Marchive D, Treheux D et al (1974) Ferritic transformation of an austenitic stainless steel by hot dipping in liquid tin or tin–nickel alloys. J Cryst Growth 24–25:559–562
21. Emmerich T, Schroer C (2017) Corrosion in austenitic steels and nickel-based alloys caused by liquid tin at high temperature. Corros Sci 120:171–183
22. Emmerich T, Durand A, Tsisar V et al (2018) Aspects of corrosion of iron- and nickel-based materials by liquid tin: oxygen dissolved in the melt and saturation with the parent element. Mater Corros 69(7):832–849
23. Heinzel A, Weisenburger A, Müller G (2017) Corrosion behavior of austenitic steel AISI 316L in liquid tin in the temperature range between 280 and 700 °C. Mater Corros 68(8):831–837
24. Mazandarany FN, Pehlke RD (1973) Thermodynamic properties of solid alloys of chromium with nickel and iron. Metall Trans 4(9):2067–2076
25. Gao Y, Takahashi M, Nomura M (2015) Characteristics of iron and nickel diffusion in molten lead–bismuth eutectic. Mech Eng J 2(6):15–00149 (9 pages)
26. Chase MW, Davies CA, Downey JR et al (1985) JANAF thermochemical tables, third edition. J Phys Chem Ref Data 14, Suppl. 1:1–1856
27. Suzuki T, Mutoh I (1989) A revisit to "steady-state corrosion rate of type 316 stainless steel in sodium in a non-isothermal loop system. J Nucl Mater 165(1):83
28. Suzuki T, Mutoh I (1988) Steady-state corrosion rate of type 316 stainless steel in sodium in a non-isothermal loop system. J Nucl Mater 152(2–3):343–347
29. Suzuki T, Mutoh I, Yagi T et al (1986) Sodium corrosion behavior of austenitic alloys and selective dissolution of chromium and nickel. J Nucl Mater 139(2):97–105
30. Lin LF, Chao CY, Macdonald DD (1981) A point defect model for anodic passive films: II. Chemical breakdown and pit initiation. J Electrochem Soc 128(6):1194–1198
31. Chao CY, Lin LF, Macdonald DD (1981) A point defect model for anodic passive films: I. Film growth kinetics. J Electrochem Soc 128(6):1187–1194
32. Alden T, Stevenson DA, Wulff J (1958) Solubility of nickel and chromium in molten lead. T Metall Soc AIME 218(2):15–17
33. Predel B (1995) Fe–Sn (Iron–Tin). In: Madelung O (ed) Dy–Er—Fr–Mo. Springer, Berlin, pp 1–5
34. Predel B (1998) Ni–Sn (Nickel–Tin). In: Madelung O (ed) Ni–Np—Pt–Zr. Springer, Berlin, pp 1–4